IEEE Access
Multidisciplinary | Rapid Review | Open Access Journal

Received February 6, 2017, accepted March 1, 2017, date of publication March 20, 2017, date of current version May 17, 2017.

Digital Object Identifier 10.1109/ACCESS.2017.2684189

Parameter Estimation of Convolutional and Helical Interleavers in a Noisy Environment

SWAMINATHAN R[1], A. S. MADHUKUMAR[1], (Senior Member, IEEE), NG WEE TECK[2], AND CHONG MENG SAMSON SEE[2], (Member, IEEE)

[1]School of Computer Science and Engineering, Nanyang Technological University, Singapore 639798
[2]Temasek Laboratories, Nanyang Technological University, Singapore 639798

Corresponding author: Swaminathan R (sramabadran@ntu.edu.sg)

ABSTRACT Forward error correction (FEC) codes followed by an interleaver play a significant role in improving the error performance of the digital systems by counteracting random and burst errors. In most of the applications, interleaver and FEC code parameters are known at the receiver to successfully de-interleave and decode the information bits. However, in certain non-cooperative applications, only partial information about the code and interleaver parameters is known. Furthermore, in cognitive radio applications, an intelligent receiver should adapt itself to the transmission parameters. Hence, there is a need to blindly estimate the FEC code and interleaver parameters in the mentioned applications from the received data stream with the availability of partial knowledge about the transmission parameters at the receiver. In this paper, a blind recognition of convolutional and helical interleaver parameters is carried out using innovative algorithms for unsynchronized, convolutionally encoded data in the presence of bit errors. In addition, the proposed algorithms also estimate the starting bit position for achieving proper synchronization. In a nutshell, it has been observed from the numerical results that the interleaver parameters have been estimated successfully over erroneous channel conditions from the proposed algorithms. Finally, the performances of the proposed algorithms for both the interleavers considering various bit error rate values have also been analyzed.

INDEX TERMS Blind recognition, convolutional interleaver, cognitive radio, forward error correction (FEC) codes, helical interleaver.

I. INTRODUCTION

To improve the error performance of the digital systems, forward error correction (FEC) codes play a significant role in nullifying the randomly distributed errors. However, if the data is communicated over burst-error channels, then the receiver will encounter significant degradation in the symbol error probability (SEP) performance. Interleaver, which follows the FEC encoder, plays a vital role in protecting the digital communication or storage systems against the burst errors, thereby improving the reliability. Therefore, both the random and burst errors are nullified by a sequential combination of FEC encoder and interleaver. Various types of interleavers such as block interleaver, helical scan interleaver, convolutional interleaver, helical interleaver, random interleaver, etc. had been designed, analyzed, and studied in the literature. In this paper, our discussions are restricted to convolutional and helical interleavers for convolutionally encoded data.

The accurate information about the code and interleaver parameters is critical to decode and de-interleave the received information symbols. However, in a non-cooperative context such as military and spectrum surveillance applications as mentioned in [1]–[3], the FEC code and interleaver parameters are either not known or only partially known at the receiver. Further, in cognitive radio applications as indicated in [4] and [5], the receiver should adapt itself to the transmission parameters. Hence, blind/semi-blind estimation is mandatory for such applications in order to successfully decode and de-interleave the received information symbols. Usually, a control channel will be used to signal the transmission parameters to the receiver in the case of adaptive modulation and coding (AMC) based systems. Thus, the blind estimation techniques at the receiver will lead to conservation of channel resources in AMC-based applications thereby improving the spectral efficiency. It is to be noted that the convolutional interleaver is prominently used in digital video broadcasting (DVB) systems [6] and possible application of helical interleaver includes interleave-division multiple access (IDMA) systems [7]. The AMC framework is

adopted in popular DVB-S2 systems [8] and wireless sensor networks [9]. The blind estimation algorithms at the receiver will reduce the energy consumption of the sensor nodes. This is because, the sensor nodes need not frequently transmit the overhead information to indicate changes in the code and interleaver parameters. Moreover, the parameter extraction techniques are also useful to identify possible error correcting codes in the genetic code of DNA sequences [10]. Since FEC codes and interleavers are extensively used in digital storage applications, the blind estimation of parameters will provide a lot of flexibility in designing the receiver decoding system.

The FEC code parameter estimation techniques were extensively studied in the literature. In [3], innovative algorithms for estimating the parameters of various FEC codes were proposed over non-erroneous scenario. In [4], [5], [11], and [12], the estimation of convolutional code parameters was carried out for erroneous scenario based on the dual code concept. In addition, the blind recognition of puncturing pattern was also proposed in [13] and [14] for punctured convolutional codes. But the estimation algorithms were limited to Galois field GF(2). However, the algorithms were extended to GF(2^m) case in [15] and [16] assuming non-binary convolutional and block codes, respectively. In [17]–[19], novel code parameter recognition techniques for low-density parity-check (LDPC) codes and convolutional codes was studied. It was observed that the proposed techniques were based on the computation of average log-likelihood ratios (LLRs) of the syndrome a posteriori probability and average likelihood difference of the parity checks. However, the LLR-based techniques are not strictly blind. This is because, a predefined set of encoders should be assumed to be known at the transmitter and receiver. The parameter estimation techniques for turbo codes based on iterative expectation-maximization and least square methods were proposed in [20] and [21], respectively.

In the prior works reported in [1], [22], and [23], innovative algorithms for the blind recognition of block interleaver parameters were discussed. In particular, the parameter estimation of block interleaver considering Hamming block code was investigated in [1]. Furthermore, the estimation of block interleaver size was carried out for non-binary coded data streams in [22]. In [23], innovative algorithms for the parameter estimation of block interleavers, which include matrix and helical scan interleavers, from convolutionally encoded data in the presence of bit errors were proposed. There are other interleaver types such as convolutional and helical interleavers whose parameter estimation techniques were not rigorously discussed in the literature. In [24] and [25], the algorithms for blind identification of convolutional interleaver parameters such as interleaver depth and width were reported for linear block coded data. The proposed algorithm in [24] to estimate the convolutional interleaver parameters was based on recognizing the data bits of a particular codeword from the row and column indices of the data matrix. However, the delay of the received data sequence to achieve synchronization was not recovered. Moreover, the proposed methodology in [24] was applicable only to block coded symbols due to its code dependent features. In [25], the algorithm was proposed for non-erroneous channel conditions. In our manuscript, we propose innovative algorithms for the blind recognition of convolutional interleaver parameters based on the rank deficiency property of convolutionally encoded data symbols [4]. Further, the delay of the received data sequence is also recovered to achieve synchronization using the proposed algorithms.

A. MOTIVATION

The main motivations behind the proposed work are as follows:

- In a non-cooperative scenario such as military and spectrum surveillance applications, it is always mandatory to recognize the coding and interleaving parameters at the receiver, as complete knowledge about the same may not be available for decoding and de-interleaving.
- In the earlier works, the proposed approach for the parameter estimation of convolutional interleaver was applicable only to block coded symbols due to its code dependent features. To the best of our knowledge, the parameter estimation of convolutional interleaver under erroneous channel conditions had not been investigated for convolutionally encoded data with and without puncturing.
- The parameter estimation was reported only for a special case assuming codeword length $n = B \times M$, where B and M denote the interleaver depth and width, respectively.
- Finally, to the extent of our knowledge, the parameter estimation of helical interleaver had not been investigated in the prior works.

B. CONTRIBUTION

The main contributions of the proposed work are as follows:

- In this paper, we assume a non-cooperative scenario, where the data symbols are encoded using convolutional codes and interleaved using convolutional or helical interleaver at the transmitter. We assume that the receiver has only a limited knowledge about the FEC codes and interleavers used at the transmitting end.
- Therefore, we propose algorithms for the blind recognition of convolutional and helical interleaver parameters in the presence of bit errors. It is to be noted that the type of interleaver is assumed to be known at the receiver.
- Unlike the prior works, the interleaver parameter estimation process is carried out for a generic case without any restriction on the codeword length n.
- Using the proposed algorithms, the convolutional interleaver parameters B and M are estimated in the presence of bit errors. In addition, the helical interleaver parameters such as the number of columns in helical array (C), group size (N), and helical array step size (d) are also estimated.

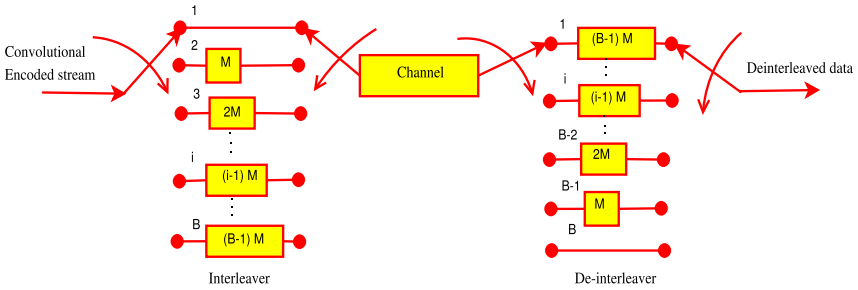

FIGURE 1. Structure of convolutional interleaver and de-interleaver considering interleaver depth B and interleaver width M.

- The identification of interleaver parameters from punctured and unpunctured convolutional codes are given for various test cases.
- Finally, by varying the bit error rate (BER) values, the performances of both the interleavers are shown for different values of constraint length K of convolutional codes.

C. STRUCTURE

The rest of the paper is organized as follows. In Section II, a brief introduction is given for both the interleavers. Section III gives an overview of the parameter estimation process with the help of a generic block diagram. In Section IV and V, the algorithms for estimating the convolutional and helical interleaver parameters are given. In addition, the complexity analysis of the proposed algorithms is also carried out in Section V. In Section VI, the simulation results and related discussions are given for various test cases. Finally, the concluding remarks are given in Section VII.

II. CONVOLUTIONAL AND HELICAL INTERLEAVERS

In the case of (B, M) convolutional interleaver, the coded data stream is stored sequentially into a bank of B registers and the i^{th} register has $(i-1)M$ delay units. With each incoming new coded symbol, the commutator switches to the subsequent register such that the new incoming symbol will be stored and the oldest symbol will be shifted out for transmission. The de-interleaver performs the inverse operation at the receiver. Note that the interleaver and de-interleaver switches should be operated synchronously. The structure of a (B, M) convolutional interleaver and de-interleaver is shown in Fig. 1. In the case of $(N_{\text{row}}, N_{\text{col}})$ block interleaver, the end-to-end delay between the restored and original sequence is $2N_{\text{row}}N_{\text{col}} - 2N_{\text{row}} + 2$ as stated in [26], where N_{row} and N_{col} indicate the number of rows and columns of the interleaver matrix, respectively. In addition, the block interleaver requires memory which can store $N_{\text{row}}N_{\text{col}}$ symbols at each end (i.e. transmitter and receiver). In the case of convolutional interleaver, the end-to-end delay and memory requirements are $B(B-1)M$ and $B/2(B-1)M$, respectively [26]. It is observed that one-half of the delay and memory requirements is reduced in the case of a (B, M) convolutional interleaver compared to a (B, BM) block interleaver which can correct burst errors of the same length.

The Helical Interleaver permutes the incoming symbols in a helical fashion by placing them in an array, which comprises of C columns and unlimited rows, and then outputs the symbols row by row to the output port. The incoming symbols are partitioned into consecutive groups of N symbols, where N is the group size parameter, and stored in an array. At each time step, the interleaver accepts an input of length CN and places the p^{th} group of N symbols in the array along $\{p \bmod C\}^{\text{th}}$ column. The placement is helical because the first symbol in the p^{th} group is in $\{1 + (p-1)d\}^{\text{th}}$ row, where d indicates the helical array step size parameter. The vacant positions in the array are filled with some default values, which is assumed to be zero in our case. The de-interleaver performs the inverse operation at the receiver. In Fig. 2, the helical

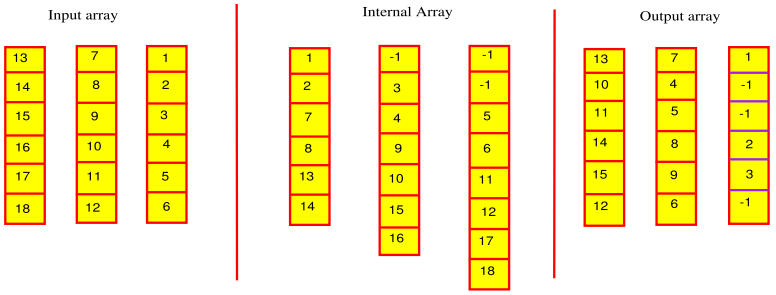

FIGURE 2. Helical interleaver [27] operation assuming $C = 3$, $N = 2$, and $d = 1$ for input values [1 : 18].

interleaver operation is shown using an example considering $C = 3$, $N = 2$, and $d = 1$ and the output of the interleaver is also shown for input values [1 : 18]. From the figure, it is observed that the interleaver outputs few symbols which are not from the current input and it leaves few symbols in the current input without placing them at the output. The helical interleaver is different from a helical scan interleaver proposed in [23]. Unlike helical interleaver, the helical scan interleaver follows block interleaving methodology which segregates the incoming data steam into multiple blocks of size equal to $N_{\text{row}}N_{\text{col}}$. In contrast to the helical interleaver, the helical scan interleaver stores the incoming symbols by filling a $N_{\text{row}} \times N_{\text{col}}$ matrix row by row and outputs all the stored symbols diagonal-wise in a helical fashion according to the step size d. The parameter estimation of block interleavers, which include matrix and helical scan interleavers, in the presence of bit errors has already been investigated in [23]. In this manuscript, our discussions are restricted to convolutional and helical interleavers.

III. INTERLEAVER PARAMETER ESTIMATION PROCESS

A generic block diagram showing the necessary blocks required to carry out the parameter estimation process considering convolutional and helical interleavers is shown in Fig. 3. After the reception of convolutionally encoded data symbols, it should be reshaped into a matrix form and the resultant matrix is termed as data matrix S. After that the difference between the number of columns of S resulting in rank deficiency, which is termed as rank-deficiency-difference, considering a particular interleaver need to be estimated. Subsequently, the estimated rank-deficiency-difference will be given as an input parameter to the algorithms which are proposed to estimate the interleaver parameters. It is to be noted that the number of bits to be shifted for achieving proper synchronization can also be estimated using the same algorithms. Finally, after estimating all the interleaver parameters, the convolutional code parameters should be estimated after de-interleaving. In this manuscript, our discussions are restricted to the parameter estimation of convolutional and helical interleavers. The code parameter estimation of convolutional codes has not been discussed here and the same has already been discussed extensively in [4], [5], and [11]–[14].

IV. RANK-DEFICIENCY-DIFFERENCE ESTIMATION

For non-erroneous scenario, the rank-deficiency-difference of convolutional or helical interleaver is estimated using algorithm 1 (refer to next page).

Algorithm 1 Rank-Deficiency-Difference Estimation

Notations: b and a indicate the number of columns and rows of data matrix S, respectively. The rank and rank ratio of S are denoted by $\rho(S)$ and p, respectively. ζ and F denotes the rank-deficiency-difference and column echelon form of S, respectively.

Assumptions: $a \geq 2b$ and the data stream is assumed to be encoded using convolutional encoder and interleaved using convolutional or helical interleaver at the transmitter.

1: The received data stream is reshaped into a data matrix S of size $a \times b$.
2: Apply Gauss-Jordan elimination through pivoting (GJETP) algorithm [28] in GF(2) and convert S into F.
3: Compute $\rho(S)$ from the number of non-zero columns in F.
4: Compute $p = \rho(S)/b$.
5: Evaluate p for different values of b.
6: Observe the difference between the successive number of columns with rank deficiency and the same gives ζ.

From algorithm 1, Gauss-Jordan elimination through pivoting (GJETP) algorithm eliminates all the dependent columns. It is also to be observed that $\zeta = \beta$ or $\zeta = \text{lcm}(n, \beta)$ for helical interleaver, where $\beta = C \times N$, and $\zeta = B$

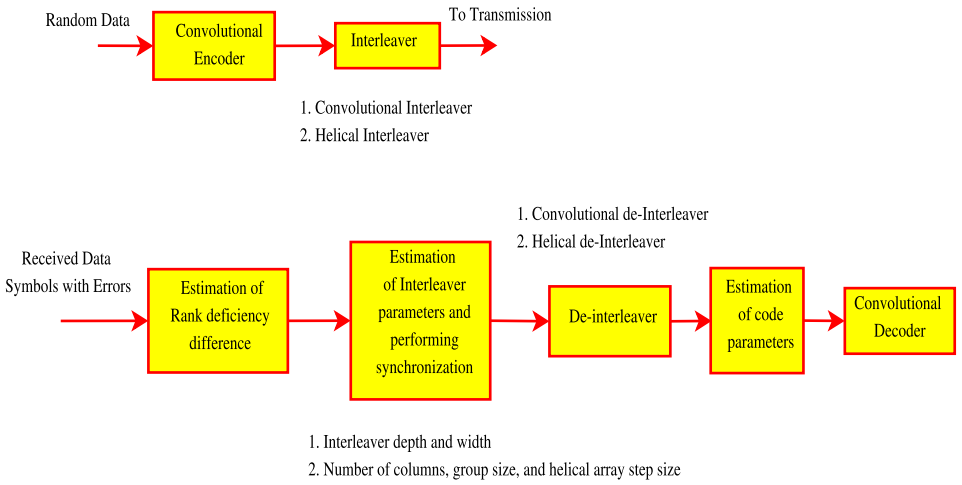

FIGURE 3. Generic block diagram for parameter estimation process of convolutional and helical interleavers.

or $\zeta = \text{lcm}(n, B)$ for convolutional interleaver. The reason for rank deficiency in the case of convolutional and helical interleavers is explained using the following propositions.

A. CONVOLUTIONAL INTERLEAVER: PROPOSITION 1

By varying b, if B is a multiple of n, then rank deficiency will be obtained for the case when $b = \alpha B$, where α is a positive integer. The deficient rank depends on the number of complete codewords contained within b. If $b = \alpha B$ and $b = \gamma n$, where γ is a positive integer, then the interleaved stream will contain less than γ complete codewords within b due to the structural properties of convolutional interleaver. For instance, if there are χ complete continuous codewords in all the rows, where $\chi < \gamma$, aligned properly in the same column, then $\rho(S)$ is given by

$$\begin{aligned}\rho(S) &= \chi k + m + (n(\gamma - \chi)) \\ &= \chi k + m + (b - \chi n),\end{aligned} \tag{1}$$

where m is the memory of the convolutional encoder, k denotes the code dimension of the convolutional codes. However, if $b \neq \alpha B$, then full rank will be obtained.

B. EXPLANATION

The data and parity bits are aligned properly in the same column only for the case when b is a multiple of B (i.e. $b = \alpha B$) assuming that B is a multiple of n. If χ complete continuous codewords in all the rows are aligned properly in the same column, then χn columns of S will be converted into $\chi k + m$ independent columns through GJETP algorithm. This is because, the output n data bits depend on $k + m$ bits (i.e. k present and m previous input bits) in the case of convolutional codes as indicated in [4] and [5]. Hence, χn output data bits or χ complete codewords in each row will depend on $\chi k + m$ input bits. Due to proper alignment of the data and parity bits, there will be only $\chi k + m$ non-zero columns after converting S into F, since GJETP algorithm will remove $(\chi n) - (\chi k + m)$ dependent columns. It is also to be noted that before applying GJETP algorithm, already S will consist of $b - \chi n$ independent columns due to incomplete codewords. Therefore, if b is a multiple of B, then $\chi k + m + b - \chi n$ non-zero columns out of b will be observed in F. Since the number of non-zero columns in F or the number of independent columns in S gives the rank of a matrix, $\rho(S)$ is given by $\chi k + m + b - \chi n$ as mentioned in (1). However, if $b \neq \alpha B$, then the data and parity bits of χ complete codewords will be segregated in different rows and will not be aligned properly in the same column. Due to improper alignment of data and parity bits, full rank will be obtained.

The above phenomenon is also explained using an example in Appendix A.

C. CONVOLUTIONAL INTERLEAVER: PROPOSITION 2

By varying b, if B is not a multiple of n, then rank deficiency will be obtained for the case when $b = \alpha \,\text{lcm}(n, B)$. Assuming $b = \gamma n$, if there are χ complete continuous codewords contained within b, where $\chi < \gamma$, then $\rho(S)$ is given by (1). However, if $b \neq \alpha \,\text{lcm}(n, B)$, then full rank will be obtained.

D. EXPLANATION

Since B is not a multiple of n, it is intuitive that the rank deficiency will be obtained when b is a multiple of $\text{lcm}(n, B)$. Rest of the explanation is similar to that of proposition 1. The proposition 2 for convolutional interleaver is also explained using an example in Appendix B.

E. HELICAL INTERLEAVER: PROPOSITION 3

Similar to convolutional interleaver, while varying b, if β is a multiple of n (i.e. $\beta = \gamma n$), then rank deficiency for helical interleaved data stream is obtained for the case when $b = \alpha\beta$. Therefore, if there are χ complete codewords, where $\chi < \gamma$, contained within b and if $b = \alpha\beta$, then $\rho(S)$ is given by (1). In addition, if β is not a multiple of n, then rank deficiency will be obtained only for the case when $b = \alpha \,\text{lcm}(n, \beta)$. However, if $b \neq \alpha\beta$ or $b \neq \alpha \,\text{lcm}(n, \beta)$, then full rank will be obtained.

The explanation for rank deficiency in the case of helical interleaver is similar to convolutional interleaver. In addition, the above phenomenon for helical interleaver is further explained using an example in Appendix C.

F. ESTIMATION OF ζ

Let $b = \alpha\beta$ and $b' = (\alpha + 1)\beta$ indicate two successive columns with rank deficiency for helical interleaver. By observing $b' - b$, $\zeta = \beta$ is estimated for helical interleaver considering the case when β is a multiple of n. For the case when β is not a multiple of n, $\zeta = \text{lcm}(n, \beta)$ is estimated by observing $b' - b$. Similarly, $\zeta = B$ or $\zeta = \text{lcm}(n, B)$ for convolutional interleaver can be estimated as mentioned in Step 6 of algorithm 1 by observing $b' - b$. The above three propositions based on the rank deficiency approach are applicable only for non-erroneous scenario. For erroneous case, S will have full rank for all values of b due to erroneous bits. It is to be noticed that the rank deficient data matrix under erroneous channel conditions will have more number of zeros compared to the full rank matrix. Therefore, the data matrix S with deficient rank will be identified by evaluating the zero-mean-ratio of column echelon form F, which is denoted by $\mu(b)$, and the same is given by

$$\mu(b) = \frac{\sum_{c=1}^{b} \sigma(c)}{b}, \tag{2}$$

where $\sigma(c) = \frac{\phi(c)}{a}$ indicates the mean value of number of zeros in c^{th} column of F and $\phi(c)$ denotes the number of zeros in c^{th} column. Now ζ will be estimated based on the values of $\mu(b)$ under erroneous channel conditions using algorithm 2.

V. ESTIMATION OF INTERLEAVER PARAMETERS

After recognizing ζ, the interleaver parameters such as B and M for convolutional interleaver and C, N, and d for helical interleaver should be estimated. In addition, the number of bit positions to be shifted for achieving proper synchronization

Algorithm 2 Estimation of ζ for Erroneous Case

Notations: $\mu'(b)$ denotes the normalized zero-mean-ratio.
Assumptions: $a \geq 2b$ and the received data stream is assumed to have bit errors.
1: Convert S into F using GJETP algorithm.
2: Evaluate $\mu(b)$ as given by (2).
3: Compute $\mu'(b)$ by normalizing $\mu(b)$ with respect to the maximum value $\mu_{\max}$. Now the normalized zero-mean-ratio $\mu'(b)$ is given by

$$\mu'(b) = \frac{\mu(b)}{\mu_{\max}}. \tag{3}$$

4: Observe the difference between the zero-dominant columns or the successive number of columns with higher values of $\mu'(b)$ and the same gives ζ for erroneous case.

should also be identified in order to de-interleave the data precisely based on the estimated interleaver parameters. Let $\phi \in [0, \zeta-1]$ denotes the bit position adjustment to achieve frame synchronization. For instance, if the receiver starts receiving the data stream at Δ^{th} bit position of t^{th} interleaver block, then frame synchronization is achieved after shifting $\phi = (t\zeta+1)-\Delta$ bit position. Since n is not known apriori, it is not possible to know whether $\zeta = B$orlcm(n, B) for convolutional interleaver and $\zeta = \beta$ or lcm(n, β) for helical interleaver. Therefore, in general, we assume that $\zeta = \text{lcm}(n, B)$ and $\zeta = \text{lcm}(n, \beta)$ are, respectively, estimated for convolutional and helical interleavers. With this assumption, an algorithm for estimating the convolutional interleaver parameters along with codeword length n is proposed (refer to algorithm 3).

In algorithm 3, we de-interleave the received data stream using (B', M') convolutional interleaver by simultaneously shifting the starting bit position ϕ of the interleaved data within 0 to $\zeta - 1$. After de-interleaving, $\delta(B', \phi, M')$ is computed for each possible combinations of $[B', \phi, M']$. For the case when $B' = B$, $M' = M$, and synchronized bit position, $\delta(B', \phi, M')$ is minimum and is equal to n. Further, for rest of the cases, $\delta(B', \phi, M') > n$. The reason is given as follows: By de-interleaving with correct interleaver and synchronization parameters, the data symbols will be convolutionally encoded. If the encoded data stream is reshaped into a matrix and if we calculate the rank of the matrix, then rank deficiency will be obtained only for the case when b is a multiple of n as mentioned in [4] and [5]. For erroneous case, full rank will be obtained irrespective of b. Therefore, $\mu'(b)$ will be evaluated for erroneous scenario. It will be observed that $\mu'(b)$ will be higher when b is a multiple of n compared to the case when b is not a multiple of n. Hence, the difference between the successive number columns with higher values of $\mu'(b)$ (i.e. $\delta(B', \phi, M')$) will be observed to be equal to n. Further, if the interleaved data is de-interleaved using incorrect parameters, then the data symbols will not be

Algorithm 3 Convolutional Interleaver

Notations: $M_{\max}$ denotes the maximum value of interleaver width, ϕ indicates the bit position adjustment to achieve synchronization, and $\delta(B', \phi, M')$ denotes the difference between the zero-dominant columns or the difference between the successive number of columns with higher values of $\mu'(b)$ for convolutional interleaver;
Assumptions: $B' > 1, M' \in [1, M_{\max}], \phi \in [0, \zeta - 1]$, $b \in [b_{\min}, b_{\max}]$;
Input: $\zeta = \text{lcm}(n, B)$;
Output: B^{est}, M^{est}, ϕ^{est} and n^{est};
1: **for** i=1:n_{max} **do**
  Get all possible unique values of B' that satisfy $\text{lcm}(i, B') = \zeta$;
end
2: For each possible combinations of $[B', \phi, M']$, de-interleave and evaluate $\mu'(b)$ for different values of b;
3: For each possible checks, obtain $\delta(B', \phi, M')$;
4: $[B^{\text{est}}, \phi^{\text{est}}, M^{\text{est}}] = \underset{B', \phi, M'}{\text{argmin}}(\delta(B', \phi, M'))$;
5: $n^{\text{est}} = \delta(B^{\text{est}}, \phi^{\text{est}}, M^{\text{est}})$;

convolutionally encoded and instead, it will be again convolutionally interleaved with rearrangement of symbol positions. Hence, when de-interleaved using incorrect parameters, it will be observed that $\delta(B', \phi, M') = \zeta$, which is usually greater than n.

Let us assume that the number of factors that satisfy $\text{lcm}(i, B') = \zeta$ is equal to R for convolutional interleaver. It is noticed that M' is varied from 1 to $M_{\max}$ and ϕ is varied from 0 to $\zeta - 1$ in the proposed algorithm. In addition, b is varied from $b_{\min}$ to $b_{\max}$. Hence, according to algorithm 3, the number of search operations T_1 required for successful estimation of convolutional interleaver parameters is given by

$$T_1 = R\,\zeta\,M_{\max}\,(b_{\max} - b_{\min}) \tag{4}$$

Next, we propose another algorithm to estimate the convolutional interleaver parameters with reduced number of search operations (refer to algorithm 4).

Algorithm 4 Convolutional Interleaver

Input: $\zeta = \text{lcm}(n, B)$;
Output: B^{est}, M^{est}, and ϕ^{est};
1: **for** i=1:n_{max} **do**
  Get all possible unique values of B' that satisfy $\text{lcm}(i, B') = \zeta$;
end
2: Fix $b = \alpha\zeta$;
3: De-interleave and evaluate zero-mean-ratio $\mu(b)$ by simultaneously varying the parameters $[B', \phi, M']$;
4: $[B^{\text{est}}, \phi^{\text{est}}, M^{\text{est}}] = \underset{B', \phi, M'}{\text{argmax}}(\mu(b))$;

The assumptions and notations given in algorithm 3 is also valid for algorithm 4. Since b is fixed as a multiple of $\zeta = \text{lcm}(n, B)$, $\mu(b)$ is maximum due to rank deficiency for $B' = B$, $M' = M$, and synchronized bit position. By de-interleaving with correct interleaver and synchronization parameters, the data symbols will be convolutionally encoded. We know that for convolutional codes, the rank deficiency will be obtained only for the case when b is a multiple of n. Since $\zeta = \text{lcm}(n, B)$ is also a multiple of n, rank deficiency will be observed when b is fixed as a multiple of ζ. Further, it has already been mentioned that $\mu(b)$ will be higher for rank deficient matrix under erroneous channel conditions. Thus, $\mu(b)$ is maximum when de-interleaved using correct interleaver parameters as mentioned in step 4 of algorithm 4.

From algorithm 4, the number of search operations T_2 required for successful estimation of convolutional interleaver parameters is given by

$$T_2 = R\,\zeta\,M_{\max} \tag{5}$$

From the computational complexity analysis of the two algorithms given for convolutional interleaver, it can be inferred that algorithm 4 is computationally efficient compared to algorithm 3, since T_1 is greater than T_2. Despite the fact that algorithm 4 is computationally efficient, additional information about n can also be extracted using algorithm 3.

To estimate the helical interleaver parameters along with n, algorithm 5 is proposed.

Algorithm 5 Helical Interleaver

Notations: $d_{\max}$ indicates the maximum value of step size d and $\delta(C', N', \phi, d')$ denotes the difference between the zero-dominant columns or the difference between the successive number of columns with higher values of $\mu'(b)$ for helical interleaver;
Assumptions: $\beta = CN$, $C' > 1$, $N' > 1$, $d' \in [1, d_{\max}]$, $b \in [b_{\min}\ ,\ b_{\max}]$, and $\phi \in [0, \zeta - 1]$;
Input: $\zeta = \text{lcm}(n, \beta)$;
Output: C^{est}, N^{est}, d^{est}, ϕ^{est}, and n^{est};
1: **for** *i=1:n_max* **do**
  Get all possible combinations of two factors C' and N' such that $C'N' = \frac{\zeta}{i}$
end
2: For each possible combinations of $[C', N', \phi, d']$, de-interleave and evaluate $\mu'(b)$ for different values of b;
3: For each possible checks, obtain $\delta(C', N', \phi, d')$;
4: $[C^{\text{est}}, N^{\text{est}}, \phi^{\text{est}}, d^{\text{est}}] = \underset{C', N', \phi, d'}{\text{argmin}}\ (\delta(C', N', \phi, d'))$;
5: $n^{\text{est}} = \delta(C^{\text{est}}, N^{\text{est}}, \phi^{\text{est}}, d^{\text{est}})$;

From algorithm 5, for the case when $C' = C$, $N' = N$, $d' = d$, and synchronized bit position, $\delta(C', N', \phi, d')$ is minimum and is equal to n and for rest of the cases, $\delta(C', N', \phi, d') > n$. Similar to convolutional interleaver, algorithm 6 is proposed to estimate the helical interleaver parameters with reduced number of search operations.

The assumptions and notations given in algorithm 5 for helical interleaver is also valid for algorithm 6. Since b is fixed as a multiple of ζ, for $C' = C$, $N' = N$, $d' = d$, and synchronized bit position, $\mu(b)$ is maximum due to rank deficiency and the reason for the same is similar to that of convolutional interleaver. Considering the parameter estimation algorithms for helical interleaver, let us assume that the number of possible combinations of two factors C' and N' that satisfy $C' \times N' = \frac{\zeta}{i}$ is equal to R'. Similarly, the helical array step size d' and ϕ are assumed to be varied from 1 to $d_{\max}$ and 0 to $\zeta - 1$, respectively. Therefore, the number of search operations T_3 and T_4 required for successful estimation of helical interleaver parameters based on algorithm 5 and 6 are, respectively, given by

$$\begin{aligned} T_3 &= R'\,\zeta\,d_{\max}(b_{\max} - b_{\min}), \\ T_4 &= R'\,\zeta\,d_{\max} \end{aligned} \tag{6}$$

Algorithm 6 Helical Interleaver

Input: $\zeta = \text{lcm}(n, \beta)$;
Output: C^{est}, N^{est}, d^{est}, and ϕ^{est};
1: **for** *i=1:n_max* **do**
  Get all possible combinations of two factors C' and N' such that $C'N' = \frac{\zeta}{i}$
end
2: Fix $b = \alpha\zeta$;
3: De-interleave and evaluate zero-mean-ratio $\mu(b)$ by simultaneously varying the parameters $[C', N', \phi, d']$;
4: $[C^{\text{est}}, N^{\text{est}}, \phi^{\text{est}}, d^{\text{est}}] = \underset{C', N', \phi, d'}{\text{argmax}}\ (\mu(b))$;

As expected, algorithm 6 is computationally efficient compared to algorithm 5 in terms of the number of search operations. However, it is to be noticed that n can also be identified along with interleaver parameters using algorithm 5.

VI. SIMULATION RESULTS AND DISCUSSIONS

The convolutional encoder is defined as $C(n, k, K)[g_1^1, \ldots, g_i^j, \ldots, g_k^n]$, where $n, k,$ and K are defined as codeword length, code dimension, and constraint length of the convolutional codes, respectively. Further, g_i^j denotes the octal representation of generator sequence between input i and output j. The present work analyzes the performance of the interleaver parameter estimation algorithms over noisy transmission environment. It is a known fact that to achieve a given quality of service (QOS), different transmission standards specify allowable BER values. We also know that convolutional interleaver is more prominently used in DVB receiver and for desirable operation of DVB receiver, the post-FEC BER requirement is 2×10^{-4} [6]. Considering the allowances of coding gain, the pre-FEC BER values will be usually greater than 10^{-3}. Hence, a safe BER value of 10^{-2} is considered in our simulation study to account the worst case scenario. Further, the performance of the proposed

algorithms is investigated for different BER values within the range of 5×10^{-3} to 6×10^{-2}. In our simulation study, we have fixed $d_{\max} = 5$ and $M_{\max} = 5$ for convolutional and helical interleavers, respectively, as well as $n_{\max} = 5$. The parameter estimation algorithms are also tested successfully for different cases as listed in Table 1.

TABLE 1. Test code set.

No.	Code rate (r)	n	k	K	g_i^j
1	1/2	2	1	3	[5,7]
2				4	[15,17]
3				5	[23,35]
4				6	[65,57]
5				6	[75,53]
6				7	[133,171]
7				8	[345,237]
8				9	[561,753]
9				10	[1167,1545]
10				11	[2335,3661]
11	1/3	3	1	4	[13,15,17]
12				7	[133,165,171]
13				11	[2353,2671,3175]
14	1/4	4	1	7	[133,171,117,165]
15				10	[1117,1365,1633,1653]
16				12	[4767 5723 6265 7455]
16	2/3	3	2	[5,4]	[23 35 0; 0 5 13]

A. SIMULATION RESULTS FOR CONVOLUTIONAL INTERLEAVER

According to algorithm 2, the normalized zero-mean-ratio $\mu'(b)$ is evaluated for different values of b as shown in Fig. 4(a). The variation of $\mu'(b)$ with respect to b before de-interleaving is shown for convolutional interleaver assuming $C(3, 1, 7)[133, 165, 171]$, BER $= 10^{-2}$, $B = 6$, $M = 3$, and $\Delta = 7$. From the figure, it is inferred that the difference between the zero-dominant columns or the difference between the successive number of columns with higher values of $\mu'(b)$ is equal to 6. According to proposition 1, if B is a multiple of n, then $\zeta = B$ and hence, ζ is identified successfully from the erroneous convolutional interleaved data. In Fig. 4(b), the variation of $\mu(b)$ is shown after de-interleaving with all possible combinations of $[B', \phi, M']$ according to algorithm 4. The possible values of B' that satisfy $\text{lcm}(i, B') = 6$, where $i = 1 : n_{\max}$, are $B' = [2, 3, 6]$. By varying B' along with M' and ϕ, where $M' \in [1, 5]$ and $\phi \in [0, 5]$, it is observed that for $B' = 6, M' = 3$, and $\phi = 0$, $\mu(b)$ reaches maximum. Since the received data stream is already synchronized with $\Delta = t\zeta + 1$, where $t = 1$ for this case, it is not necessary to shift the bit position (i.e. $\phi = 0$). Hence, the synchronization parameter and the convolutional interleaver parameters are estimated successfully using algorithm 4.

According to algorithm 3, for each possible combinations of $[B', \phi, M']$, the coded data symbols are de-interleaved and $\mu'(b)$ is evaluated for different values of b in Fig. 5. In Fig. 5(a), the variation of $\mu'(b)$ with respect to b after de-interleaving using correct interleaver and synchronization parameters (i.e. $B' = 6$, $M' = 3$, and $\phi = 0$) is shown. It is observed that the difference between the successive number of columns with higher values of $\mu'(b)$ is equal to 3, which is the codeword length of the convolutional code assumed in this case. In Fig. 5(b), Fig. 6(a), and Fig. 6(b), the variation of $\mu'(b)$ with respect to b is shown by de-interleaving using incorrect possible combinations of $[B', \phi, M']$. From the figures, it is inferred that after de-interleaving

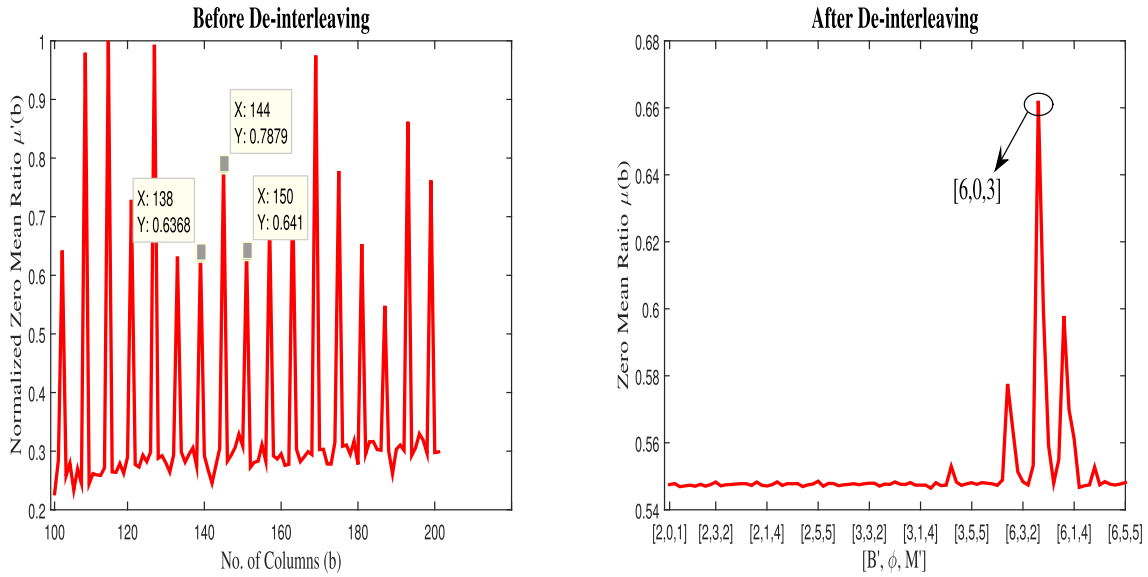

(a) (b)

FIGURE 4. (a) Variation of $\mu'(b)$ with respect to b before de-interleaving for convolutional interleaver assuming $C(3, 1, 7)[133, 165, 171]$, BER $= 10^{-2}$, $B = 6$, $M = 3$, $\Delta = 7$. (b) Variation of $\mu(b)$ by de-interleaving using all possible combinations of $[B', \phi, M']$ assuming $C(3, 1, 7)[133, 165, 171]$, BER $= 10^{-2}$, $B = 6$, $M = 3$, $\Delta = 7$.

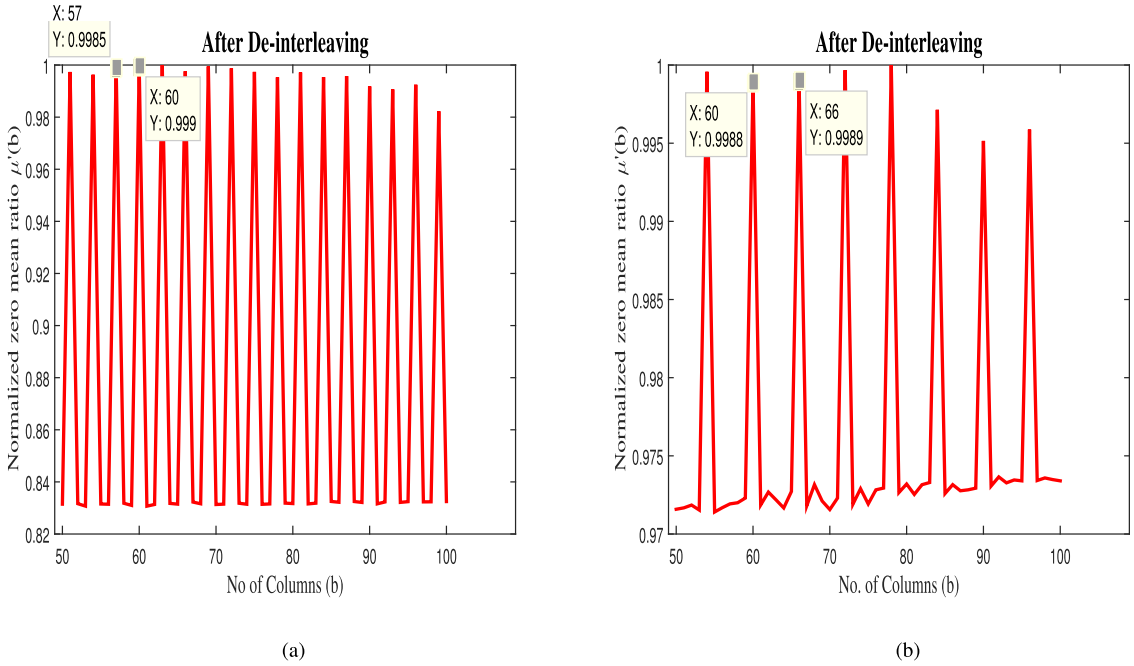

FIGURE 5. (a) Variation of $\mu'(b)$ with respect to b after de-interleaving using $[B', \phi, M'] = [6, 0, 3]$ assuming $C(3, 1, 7)[133, 165, 171]$, BER $= 10^{-2}$, $B = 6$, $M = 3$, $\Delta = 7$. (b) Variation of $\mu'(b)$ with respect to b after de-interleaving using $[B', \phi, M'] = [6, 2, 3]$ assuming $C(3, 1, 7)[133, 165, 171]$, BER $= 10^{-2}$, $B = 6$, $M = 3$, $\Delta = 7$.

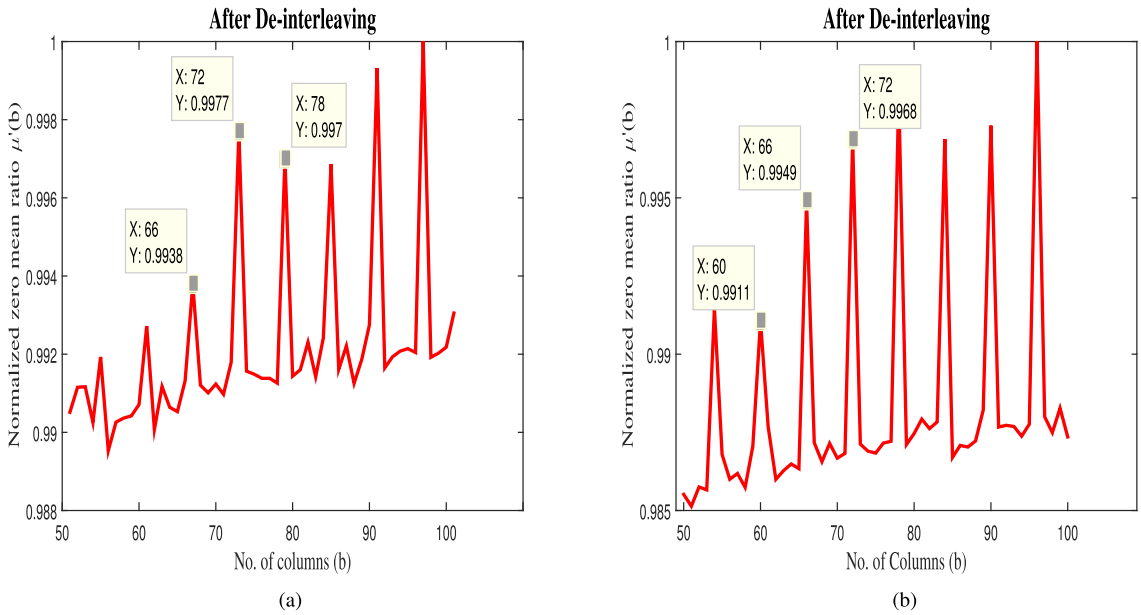

FIGURE 6. (a) Variation of $\mu'(b)$ with respect to b after de-interleaving using $[B', \phi, M'] = [2, 3, 3]$ assuming $C(3, 1, 7)[133, 165, 171]$, BER $= 10^{-2}$, $B = 6$, $M = 3$, $\Delta = 7$. (b) Variation of $\mu'(b)$ with respect to b after de-interleaving using $[B', \phi, M'] = [3, 4, 3]$ assuming $C(3, 1, 7)[133, 165, 171]$, BER $= 10^{-2}$, $B = 6$, $M = 3$, $\Delta = 7$.

using inaccurate parameters, $\delta(B', \phi, M')$ is observed to be equal to ζ, where $\zeta = 6$, which is greater than n. Note that among 90 possible combinations of $[B', \phi, M']$, we have shown only 3 combinations. It is also observed that for the rest of the incorrect possible combinations, $\delta(B', \phi, M') = \zeta$. Therefore, the interleaver and synchronization parameters for which $\delta(B', \phi, M')$ is minimum are $B' = 6$, $M' = 3$, and $\phi = 0$. It is also observed that the estimated parameters exactly match with the parameters successfully identified using algorithm 4 shown in Fig. 4.

In Fig. 7(a) and Fig. 7(b), the convolutional interleaver parameter estimation is carried out based on the

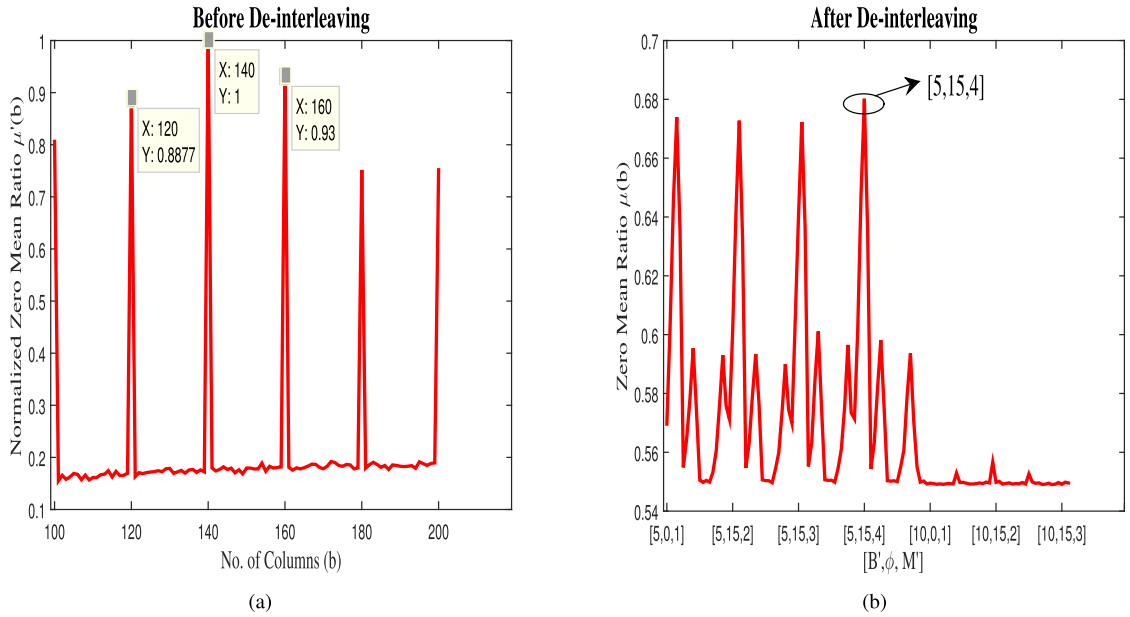

FIGURE 7. (a) Variation of $\mu'(b)$ with respect to b before de-interleaving for convolutional interleaver assuming $C(4, 1, 12)[4767, 5723, 6265, 7455]$, $B = 5$, $M = 4$, BER $= 10^{-2}$, and $\Delta = 6$. (b) Variation of $\mu(b)$ after de-interleaving with all possible combinations of $[B', \phi, M']$ assuming $C(4, 1, 12)[4767, 5723, 6265, 7455]$, BER $= 10^{-2}$, $B = 5$, $M = 4$, and $\Delta = 6$.

algorithms 2 and 4, respectively, with BER $= 10^{-2}$ assuming $C(4, 1, 12)[4767, 5723, 6265, 7455]$, $B = 5$, $M = 4$, $BER = 10^{-2}$, and $\Delta = 6$. From Fig. 7(a), it is observed that the difference between the successive number of columns with higher values of $\mu'(b)$ is equal to 20 (i.e. lcm(n, B)) according to proposition 2. Hence, ζ is successfully estimated for the case when B is not a multiple of n. In Fig. 7(b), the variation of $\mu(b)$ is shown for all possible combinations of $[B', \phi, M']$ and it is noticed that the convolutional interleaver parameters $B^{\text{est}} = 5$, $M^{\text{est}} = 4$, and the number of bits to be shifted for achieving proper frame synchronization (i.e. $\phi^{\text{est}} = 15$) are estimated successfully.

In Fig. 8(a), $\mu'(b)$ is evaluated for convolutional interleaver based on algorithm 2 and the variation with respect to b is shown for punctured convolutional code assuming $C(2, 1, 3)[5, 7]$, BER $= 10^{-2}$, $B = 4$, $M = 2$, $\Delta = 6$, and puncturing pattern $=$ [1;1;0;1]. Firstly, the zero-dominant-column difference ζ as indicated in the figure is observed to be equal to 12. After puncturing using the pattern [1;1;0;1], rate $\frac{1}{2}$ convolutional code will be converted into rate $\frac{2}{3}$ code, where punctured codeword length $n_p = 3$ and punctured input bits $k_p = 2$. Therefore, $\zeta =$ lcm(n_p, B) instead of lcm(n, B). Fig. 8(b) shows the variation of $\mu(b)$ for all possible combinations of $[B', \phi, M']$. As expected, using algorithm 4, the convolutional interleaver parameters $B^{\text{est}} = 4$, $M^{\text{est}} = 2$ and synchronization parameter $\phi^{\text{est}} = 7$ are detected successfully from the punctured convolutional code.

B. SIMULATION RESULTS FOR HELICAL INTERLEAVER

In Fig. 9(a), $\mu'(b)$ for helical interleaver is computed based on algorithm 2 and the variation of $\mu'(b)$ with respect to b is shown for $C(2, 1, 5)[23, 35]$, BER $= 10^{-2}$, $C = 3$, $N = 2$, $d = 5$, and $\Delta = 5$. Since $\beta = C \times N = 6$ is a multiple of $n = 2$, it is observed that the successive difference between the number of columns with higher values of $\mu'(b)$ is equal to β according to proposition 3. Therefore, ζ, which is equal to β for this case, is estimated correctly. In Fig. 9(b), the variation of $\mu(b)$ is shown by de-interleaving with all possible combinations of two factors C' and N' that satisfy $\frac{6}{i}$ as indicated in step 1 of algorithm 6. The de-interleaving is performed together with varying d' from 1 to 5 and ϕ from 0 to 5. From the figure, it is observed that for $C' = 3$, $N' = 2$, $d' = 5$, and $\phi = 2$, $\mu(b)$ reaches maximum. Therefore, by shifting 2 bit positions (i.e. $(t\ \zeta + 1) - \Delta$ positions, where $t = 1$), synchronization is achieved and with $C^{est} = 3$, $N^{est} = 2$, and $d^{est} = 5$, the helical interleaved data stream can be successfully de-interleaved using algorithm 6.

In Fig. 10(a), the variation of $\mu'(b)$ with respect to b after de-interleaving using correct helical interleaver and synchronization parameters (i.e. $C' = 3, N' = 2, d' = 5$, and $\phi = 2$) is shown. According to algorithm 5 proposed for helical interleaver, it is inferred from the figure that $\delta(C', N', \phi, d') = n$, where $n = 2$ for this case. In Fig. 10(b), the variation of $\mu'(b)$ is shown by de-interleaving using incorrect parameters and it is noticed that $\delta(C', N', \phi, d') = \zeta$, where $\zeta = 6$. It is also observed that for other incorrect possible combinations, $\delta(C', N', \phi, d') = \zeta$. Hence, according to step 4 in algorithm 5, the interleaver and synchronization parameters for which $\delta(C', N', \phi, d')$ is minimum are $C' = 3$, $N' = 2$, $d' = 5$, and $\phi = 2$. Thus, the estimated parameters exactly agree with the true helical interleaver parameters used for transmission.

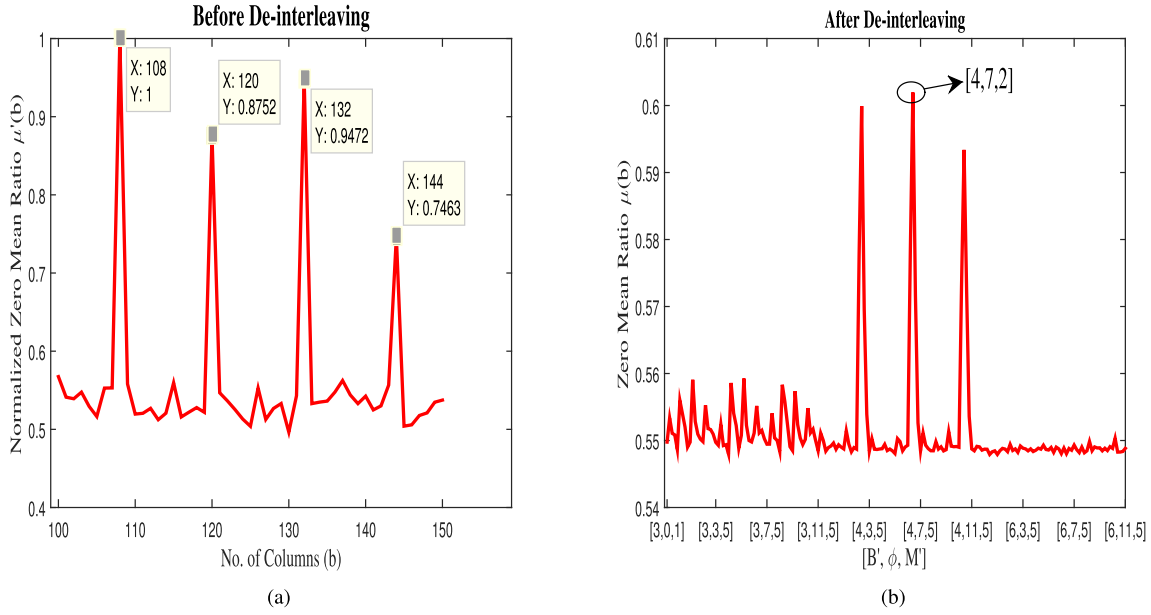

FIGURE 8. (a) Variation of $\mu'(b)$ with respect to b before de-interleaving for convolutional interleaver assuming $C(2, 1, 3)[5, 7]$, BER $= 10^{-2}$, $B = 4$, $M = 2$, $\Delta = 6$, puncturing pattern = [1;1;0;1]. (b) Variation of $\mu(b)$ after de-interleaving with all possible combinations of $[B', \phi, M']$ assuming $C(2, 1, 3)[5, 7]$, BER $= 10^{-2}$, $B = 4$, $M = 2$, $\Delta = 6$, puncturing pattern = [1;1;0;1].

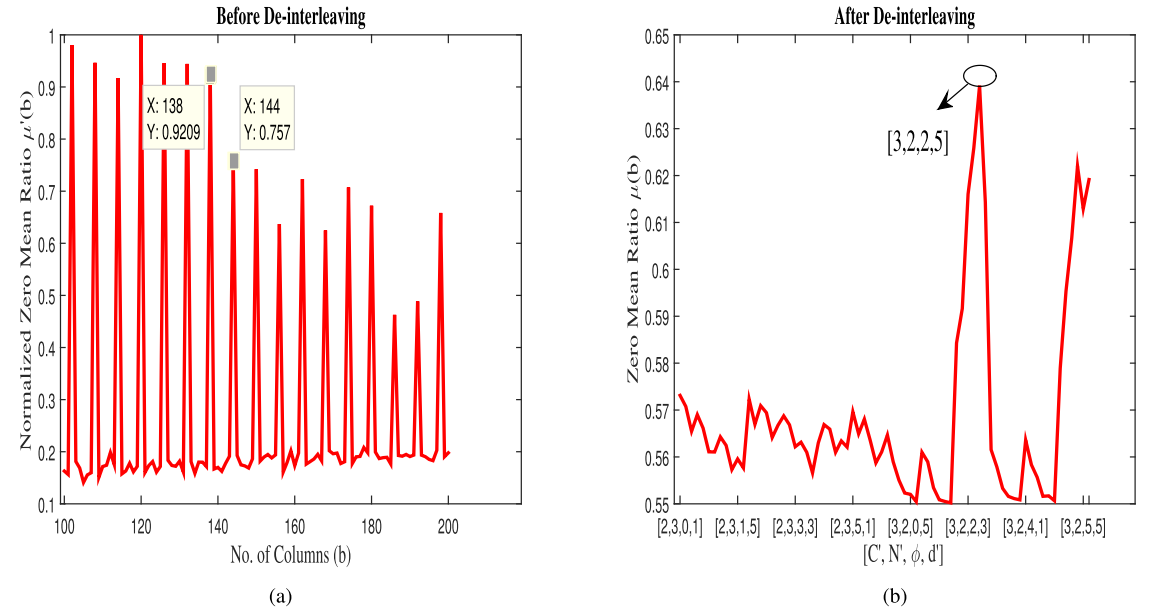

FIGURE 9. (a) Variation of $\mu'(b)$ with respect to b before de-interleaving for helical interleaver assuming $C(2, 1, 5)[23, 35]$, BER $= 10^{-2}$, $C = 3$, $N = 2$, $d = 5$, $\Delta = 5$. (b) Variation of $\mu(b)$ after de-interleaving using all possible combinations of $[C', N', \phi, d']$ assuming $C(2, 1, 5)[23, 35]$, BER $= 10^{-2}$, $C = 3$, $N = 2$, $d = 5$, $\Delta = 5$.

Fig. 11(a) and Fig. 11(b) show the zero-mean-ratio plots before and after de-interleaving, respectively, for helical interleaver considering $C(3, 1, 11)[2353, 2671, 3175]$ with $C = 5, N = 3, d = 3$, BER $= 10^{-2}$, and $\Delta = 9$. Since β is a multiple of n, $\zeta = \beta$ according to proposition 3. It is inferred from Fig. 11(a) that $\zeta = 15$ has been identified successfully using algorithm 2. In Fig. 11(b), the variation of $\mu(b)$ is shown by de-interleaving with all possible combinations of two factors C' and N' that satisfy $\frac{15}{i}$ as mentioned in step 1 of algorithm 6. The de-interleaving is performed together with varying d' from 1 to 5 and ϕ from 0 to 14. It is noticed from the figure that for $C' = 5$, $N' = 3$, $d' = 3$, and $\phi = 7$, $\mu(b)$ reaches maximum. Therefore, the helical interleaver parameters are estimated successfully using algorithm 6. Further, the incoming data stream is also synchronized by appropriately shifting correct number of bit positions.

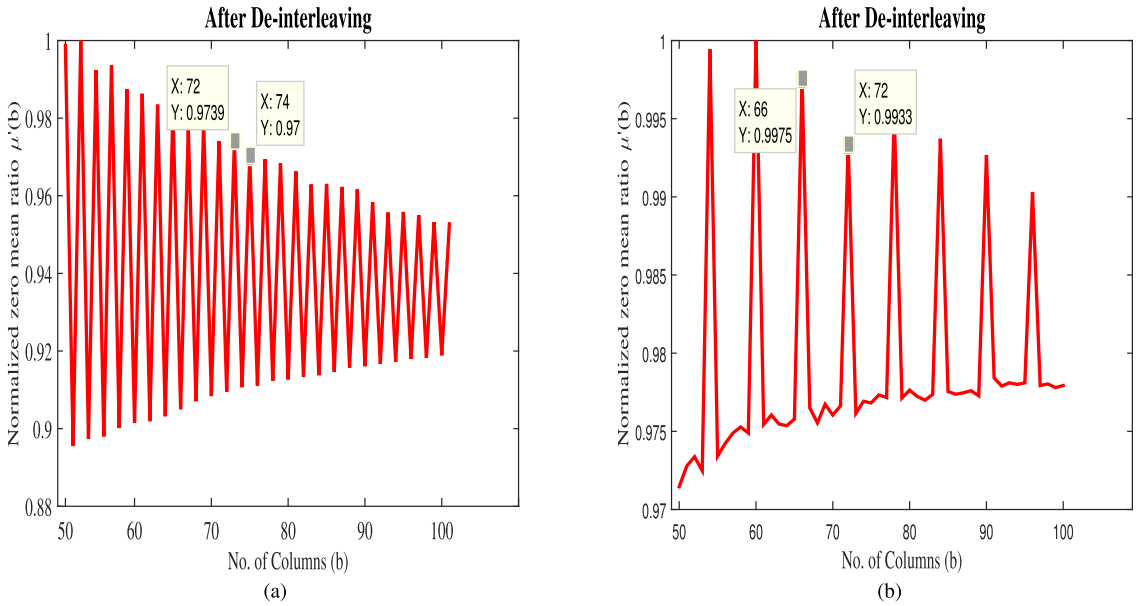

FIGURE 10. (a) Variation of $\mu'(b)$ with respect to b after de-interleaving using $[C', N', \phi, d'] = [3, 2, 2, 5]$ assuming $C(2, 1, 5)[23, 35]$, BER $= 10^{-2}$, $C = 3$, $N = 2$, $d = 5$, $\Delta = 5$. (b) Variation of $\mu'(b)$ with respect to b after de-interleaving using $[C', N', \phi, d'] = [2, 3, 2, 3]$ assuming $C(2, 1, 5)[23, 35]$, BER $= 10^{-2}$, $C = 3$, $N = 2$, $d = 5$, $\Delta = 5$.

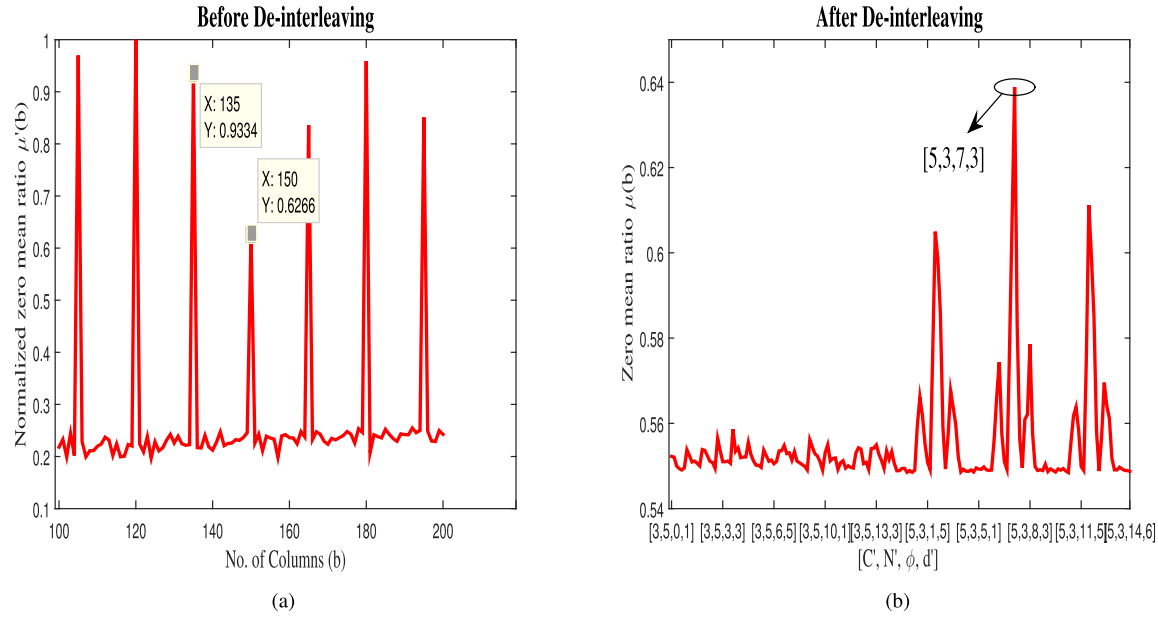

FIGURE 11. (a) Variation of $\mu'(b)$ with respect to b before de-interleaving for helical interleaver assuming $C(3, 1, 11)[2353, 2671, 3175]$, BER $= 10^{-2}$, $C = 5$, $N = 3$, $d = 3$, $\Delta = 9$. (b) Variation of $\mu(b)$ after de-interleaving using all possible combinations of $[C', N', \phi, d']$ assuming $C(3, 1, 11)[2353, 2671, 3175]$, BER $= 10^{-2}$, $C = 5$, $N = 3$, $d = 3$, $\Delta = 9$.

In Fig. 12(a), the variation of $\mu'(b)$ with respect to b is for helical interleaver assuming punctured convolutional code $C(2, 1, 3)[5, 7]$ with puncturing pattern = [1;1;0;1;1;0], $BER = 10^{-2}$, $C = 4$, $N = 4$, $d = 2$, $\Delta = 9$, $k_p = 3$, and $n_p = 4$. From the figure, ζ is observed to be equal to 16. Since β is a multiple of n_p, $\zeta = \beta$ has been identified correctly using algorithm 2. Fig. 12(b) shows the variation of $\mu(b)$ for all possible combinations of $[C', N', \phi, d']$. Using algorithm 6, the helical interleaver parameters $C^{\text{est}} = 4$, $N^{\text{est}} = 4$, $d^{\text{est}} = 2$ and synchronization parameter $\phi^{\text{est}} = 8$ are detected successfully from the punctured convolutional code, since $\mu(b)$ is maximum for $[C', N', \phi, d'] = [4, 4, 8, 2]$.

C. ACCURACY OF ESTIMATION OF BOTH THE INTERLEAVERS

In Fig. 13(a) and Fig. 13(b), the probability of correct detection of interleaver parameters is shown against

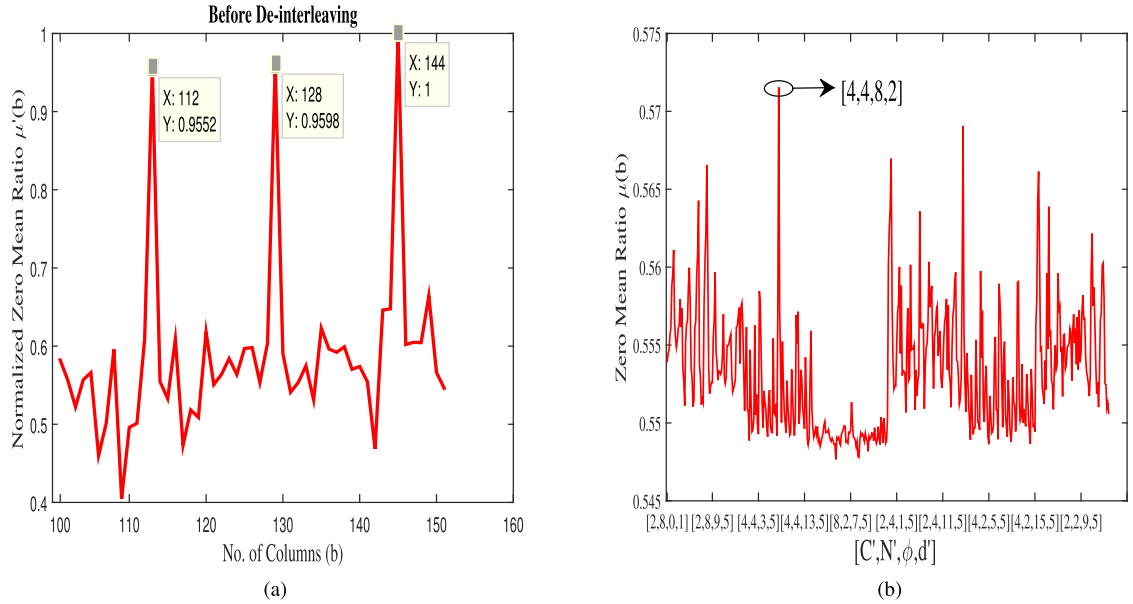

FIGURE 12. (a) Variation of $\mu'(b)$ with respect to b for helical interleaver assuming $C(2, 1, 3)[5, 7]$, BER $= 10^{-2}$, $C = 4$, $N = 4$, $d = 2$, $\Delta = 9$, puncturing pattern = [1;1;0;1;1;0]. (b) Variation of $\mu(b)$ for all possible values of $[C', N', \phi, d']$ assuming $C(2, 1, 3)[5, 7]$, BER $= 10^{-2}$, $C = 4$, $N = 4$, $d = 2$, $\Delta = 9$, puncturing pattern = [1;1;0;1;1;0].

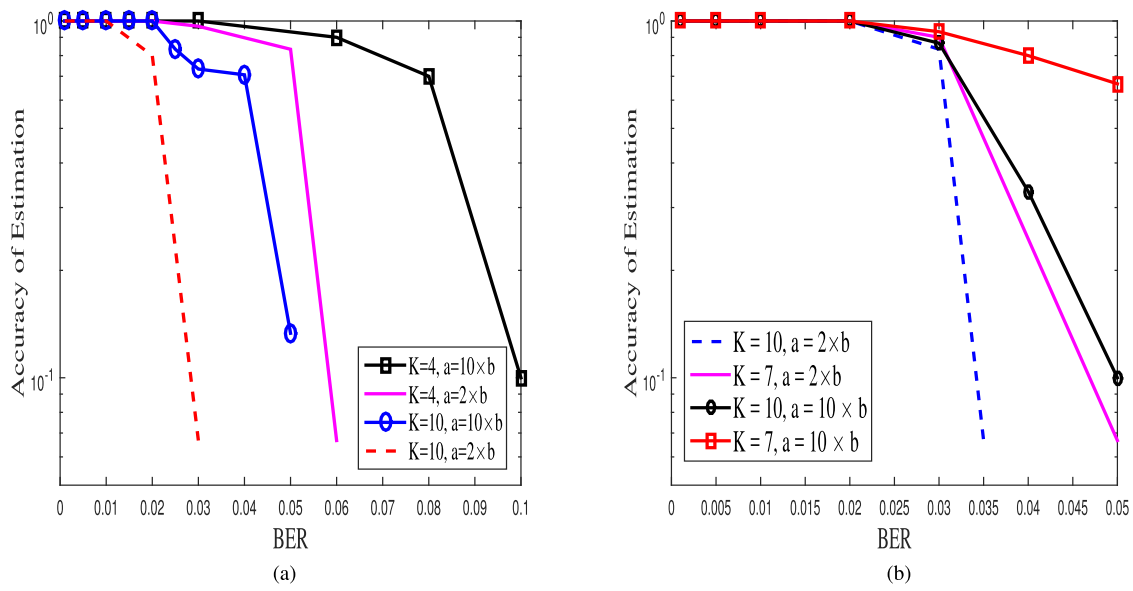

FIGURE 13. (a) Performance of convolutional interleaver ($C(3, 1, 4)[13, 15, 17]$, $C(3, 1, 7)[133, 165, 171]$, $B = 3$ and $M = 2$). (b) Performance of helical interleaver ($C(4, 1, 7)[133, 171, 117, 165]$, $C(4, 1, 10)[1117, 1365, 1633, 1653]$, $C = 4$, $N = 3$, and $d = 2$).

BER considering different values of K for convolutional and helical interleavers, respectively. Firstly, from the figures it can be observed that as K increases, the probability of estimating the interleaver parameters decreases for both the interleavers and the trend remains the same irrespective of the interleaver parameters and r. Moreover, when the number of rows a of data matrix S increases with respect to the number of columns b from $a = 2 \times b$ to $a = 10 \times b$, the probability of detecting the correct interleaver parameters also increases as expected. By averaging more number of rows, the difference between the zero-dominant columns can be predicted more accurately to estimate ζ without any intermediate peaks and hence, the estimation improves with increase in the data size. It is also to be noted that the estimation of ζ plays a vital role in estimating the interleaver parameters. Further, as K increases, the rank value associated with a particular value of b also increases as mentioned in [4] and [5]. Hence, the number of dependent columns decreases, which in turn

decreases $\mu'(b)$ for erroneous case. If $\mu'(b)$ is very less for a rank deficient column, then the accuracy in predicting ζ or the difference between the zero-dominant columns deteriorates for higher constraint length case due to the existence of intermediate peaks.

VII. CONCLUSION

In this paper, the parameter estimation of helical and convolutional interleavers is investigated in a noisy transmission environment considering convolutionally encoded data. A generic block diagram explaining the estimation process is given. Then algorithms for estimating the rank-deficiency-difference are proposed for non-erroneous and erroneous channel conditions. Further, based on the estimated value of rank-deficiency-difference, more algorithms are given for estimating the parameters of convolutional and helical interleavers. Using the proposed algorithms, bit position adjustment is also identified for achieving proper frame synchronization. From the numerical results, it is observed that the interleaver parameters are estimated successfully with 100% accuracy until BER of 2×10^{-2}. In addition, the interleaver parameters are also correctly estimated from the punctured convolutionally encoded data. Finally, the accuracy of estimation of the proposed algorithms is shown by varying the BER values for two different values of constraint length and number of rows of the data matrix. From the performance plots, an improvement in the estimation accuracy of the interleaver parameters is observed with decrease in the constraint length and increase in the data size.

APPENDIX A
CASE STUDY 1: CONVOLUTIONAL INTERLEAVER

In this Appendix, the reason for rank deficiency considering the case when B is a multiple of n as mentioned in proposition 1 for convolutional interleaver has been explained using an example. Firstly, Fig. 14 shows the variation of $\rho(S)$ with b for convolutional interleaver considering $C(2, 1, 3)[5, 7]$, $B = 2$, and $M = 2$ for non-erroneous and synchronized scenario. Note that $\rho(S)$ is computed based on algorithm 1. Let us denote the output codewords of rate 1/2 convolutional codes corresponding to the input symbols $A, B, \cdots, X, \cdots, a, b, c$ as $A_1A_2, B_1B_2, \cdots, X_1X_2, \cdots, a_1a_2, b_1b_2, c_1c_2$, respectively. In Table 2, the output codewords are convolutionally interleaved and reshaped into a data matrix S of size $a \times b$ assuming $b = 14$, 15, and 16 with number of rows $a = 3$. It is to be noted that the convolutional interleaving operation is carried out as shown in Fig. 1. For better understanding, we have shown only three rows. From the interleaved data stream, $\chi = 5$ complete continuous codewords (i.e. $H_1H_2, I_1I_2, J_1J_2, K_1K_2, L_1L_2$ in the second row and $O_1O_2, P_1P_2, Q_1Q_2, R_1R_2, S_1S_2$ in the third row) are observed. It is also noticed that all 5 complete continuous codewords are aligned properly in the same column. As χn output data bits or χ codewords depend on $\chi k + m$ input bits for convolutional codes as mentioned in [4] and [5], here, $\chi = 5$ complete continuous codewords or $\chi \times n = 10$ output data bits depend on 5 present and 2 previous bits. We assume $K = 3$ for this case and $m = K - 1$ for rate 1/n convolutional codes. Therefore, when the convolutionally interleaved data matrix S is converted into column echelon form F through GJETP algorithm, 10 columns will be converted into 7 (i.e. $\chi k+m$) non-zero columns. This is because, GJETP algorithm eliminates all the dependent columns. Moreover, it is also observed in Table 2 that there are 4 incomplete codewords which are segregated in different rows and are not aligned properly in the same column. This will result in another 4 (i.e. $b - \chi n$) non-zero columns in F. Hence, after Gauss elimination process, column echelon form of S will consist of 11 non-zero columns for the case when $b = 14$. Since the number of non-zero columns in F indicates the rank of a matrix, $\rho(S) = \chi k+m+b-\chi n$ (refer to (1)) as mentioned in proposition 1. Note that the number of independent columns in S or the number of non-zero columns in F gives the rank of a matrix.

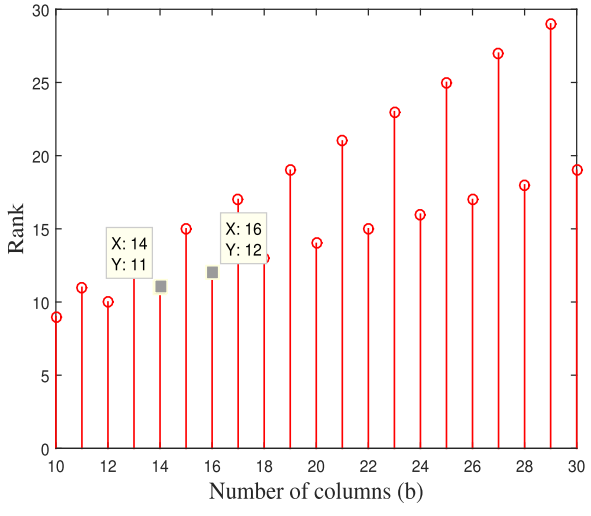

FIGURE 14. Variation of rank with number of columns (b) for convolutional interleaver ($C(2, 1, 3)[5, 7]$, $B = 2$, $M = 2$, BER = 0).

In Table 2, the convolutionally interleaved data stream for the case when $b = 16$ assuming $r = \frac{1}{2}$, $B = 2$, and $M = 2$ is also shown considering synchronized and non-erroneous scenario. Similar to $b = 14$ case, here, $\chi = 6$ continuous complete codewords are observed (i.e. $I_1I_2, J_1J_2, K_1K_2, L_1L_2, M_1M_2, N_1N_2$ in the second row and $Q_1Q_2, R_1R_2, S_1S_2, T_1T_2, U_1U_2, V_1V_2$ in the third row are aligned properly in the same column). Hence, after converting S into F, 12 columns (i.e. χn) will be reduced to 8 non-zero columns ($\chi k + m$) for the case when $K = 3$. Furthermore, there are 4 incomplete codewords (i.e. $b - \chi n$) which are segregated in different rows and the same will result in 4 non-zero columns in F. So totally 12 (i.e. $\chi k + m + b - \chi n$) non-zero columns will be observed out of 16 in F or $\rho(S) = 12$, which justifies (1) given in proposition 1.

Since b is a multiple of B, rank deficiency is observed for the cases when $b = 14$ and $b = 16$. In Table 2,

TABLE 2. Convolutionally interleaved data stream assuming $B = 2$ and $M = 2$.

$b=14$	A_1	0	B_1	0	C_1	A_2	D_1	B_2	E_1	C_2	F_1	D_2	G_1	E_2		
	H_1	F_2	I_1	G_2	J_1	H_2	K_1	I_2	L_1	J_2	M_1	K_2	N_1	L_2		
	O_1	M_2	P_1	N_2	Q_1	O_2	R_1	P_2	S_1	Q_2	T_1	R_2	V_1	S_2		
$b=16$	A_1	0	B_1	0	C_1	A_2	D_1	B_2	E_1	C_2	F_1	D_2	G_1	E_2	H_1	F_2
	I_1	G_2	J_1	H_2	K_1	I_2	L_1	J_2	M_1	K_2	N_1	L_2	O_1	M_2	P_1	N_2
	Q_1	O_2	R_1	P_2	S_1	Q_2	T_1	R_2	U_1	S_2	V_1	T_2	W_1	U_2	X_1	V_2
$b=15$	A_1	0	B_1	0	C_1	A_2	D_1	B_2	E_1	C_2	F_1	D_2	G_1	E_2	H_1	
	F_2	I_1	G_2	J_1	H_2	K_1	I_2	L_1	J_2	M_1	K_2	N_1	L_2	O_1	M_2	
	P_1	N_2	Q_1	O_2	R_1	P_2	S_1	Q_2	T_1	R_2	U_1	S_2	V_1	T_2	W_1	

convolutionally interleaved data stream is also shown for the case when $b = 15$, which is not a multiple of B. Even though there are 5 continuous complete codewords in a single row (i.e. $I_1I_2, J_1J_2, K_1K_2, L_1L_2, M_1M_2$ in the second row and $P_1P_2, Q_1Q_2, R_1R_2, S_1S_2, T_1T_2$ in the third row), all the codewords are not aligned correctly in the same column unlike $b = 14$ and $b = 16$ cases. This will result in full rank as mentioned in proposition 1.

Further, the rank values obtained for the case when $b = 14, 15,$ and 16 in this case study well agree with the rank values shown in Fig. 14. It is to be noted that the difference between two successive columns with rank deficiency is observed to be equal to 2 (i.e. B). Therefore, from Table 2 and Fig. 14, it is observed that if b is a multiple of B, then rank deficiency is obtained and $\rho(S) = \chi k + m + b - \chi n$. However, if b is not a multiple of B, then full rank is obtained.

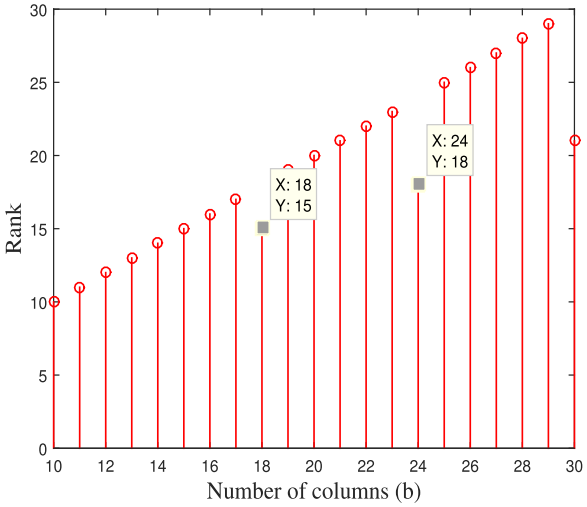

FIGURE 15. Variation of rank with number of columns (b) for convolutional interleaver ($C(2, 1, 3)[5, 7]$, $B = 3$, $M = 2$, BER = 0).

APPENDIX B
CASE STUDY 2: CONVOLUTIONAL INTERLEAVER

In this Appendix, the reason for rank deficiency considering the case when B is not a multiple of n as mentioned in proposition 2 for convolutional interleaver has been explained using an example. Here, the convolutionally interleaved data stream assuming $r = \frac{1}{2}$, $B = 3$ and $M = 2$ for the case when $b = 18$, $b = 20$, and $b = 24$ with $a = 3$ is shown in Table 3 for synchronized and non-erroneous scenario. Moreover, the variation of $\rho(S)$ with b for convolutional interleaver considering $C(2, 1, 3)[5, 7]$, $B = 3$, and $M = 2$ is shown in Fig. 15 by varying b from 10 to 30 and $\rho(S)$ is evaluated using algorithm 1. From Table 3, $\chi = 5$ complete continuous codewords are observed in the second and third rows. Since all are aligned properly in the same column, rank deficiency will be observed. Therefore, after converting S into F, $\chi = 5$ complete continuous codewords which will occupy 10 columns (i.e. $\chi \times n$) will be reduced to 7 non-zero columns (i.e. $\chi k + m$). In addition, there are 8 independent columns in S (i.e. $b - \chi n$) due to 8 incomplete codewords in a particular row as observed in Table 3. Therefore, out of 18 columns, 15 non-zero columns (i.e. $\chi k + m + b - \chi n$) will be noticed in F and hence, $\rho(S) = 15$. Similarly, for the case when $b = 24$, $\chi = 8$ complete continuous codewords are observed in a single row and are aligned properly in the same column. After applying GJETP algorithm, $\chi = 8$ complete continuous codewords which will occupy 16 columns (i.e. $\chi \times n$) will be reduced to 10 non-zero columns (i.e. $\chi k + m$). Furthermore, there are 8 incomplete codewords (i.e. $b - \chi n$) which are segregated in different rows and the same will result in 8 non-zero columns in F. So totally 18 (i.e. $\chi k + m + b - \chi n$) non-zero columns will be observed out of 24 in F or $\rho(S) = 18$ for the case when $b = 24$. Therefore, the deficient rank values obtained for $b = 18$ and $b = 24$ validate (1).

In Table 3, the convolutionally interleaved stream is also shown for the case when $b = 20$. Since all the complete codewords are not aligned in the same column, full rank will be obtained. Similar to the previous case study, the rank values obtained for the case when $b = 18, 20,$ and 24 well

TABLE 3. Convolutionally interleaved data stream assuming $B = 3$ and $M = 2$.

$b=18$	A_1	0	0	B_2	0	0	D_1	A_2	0	E_2	C_1	0	G_1	D_2	B_1	H_2	F_1	C_2						
	J_1	G_2	E_1	K_2	I_1	F_2	M_1	J_2	H_1	N_2	L_1	I_2	P_1	M_2	K_1	Q_2	O_1	L_2						
	S_1	P_2	N_1	T_2	R_1	O_2	V_1	S_2	Q_1	W_2	U_1	R_2	Y_1	V_2	T_1	Z_2	X_1	U_2						
$b=24$	A_1	0	0	B_2	0	0	D_1	A_2	0	E_2	C_1	0	G_1	D_2	B_1	H_2	F_1	C_2	J_1	G_2	E_1	K_2	I_1	F_2
	M_1	J_2	H_1	N_2	L_1	I_2	P_1	M_2	K_1	Q_2	O_1	L_2	S_1	P_2	N_1	T_2	R_1	O_2	V_1	S_2	Q_1	W_2	U_1	R_2
	Y_1	V_2	T_1	Z_2	X_1	U_2	b_1	Y_2	W_1	c_2	a_1	X_2	e_1	b_2	Z_1	f_2	d_1	a_2	h_1	e_2	c_1	i_2	g_1	d_2
$b=20$	A_1	0	0	B_2	0	0	D_1	A_2	0	E_2	C_1	0	G_1	D_2	B_1	H_2	F_1	C_2	J_1	G_2				
	E_1	K_2	I_1	F_2	M_1	J_2	H_1	N_2	L_1	I_2	P_1	M_2	K_1	Q_2	O_1	L_2	S_1	P_2	N_1	T_2				
	R_1	O_2	V_1	S_2	Q_1	W_2	U_1	R_2	Y_1	V_2	T_1	Z_2	X_1	U_2	b_1	Y_2	W_1	c_2	a_1	X_2				

TABLE 4. Helical interleaved data stream assuming $C = 3$, $N = 2$, and $d = 1$.

$b=12$	A_1	0	0	A_2	B_1	0	D_1	B_2	C_1	D_2	E_1	C_2						
	G_1	E_2	F_1	G_2	H_1	F_2	J_1	H_2	I_1	J_2	K_1	I_2						
	M_1	K_2	L_1	M_2	N_1	L_2	P_1	N_2	O_1	P_2	Q_1	O_2						
$b=18$	A_1	0	0	A_2	B_1	0	D_1	B_2	C_1	D_2	E_1	C_2	G_1	E_2	F_1	G_2	H_1	F_2
	J_1	H_2	I_1	J_2	K_1	I_2	M_1	K_2	L_1	M_2	N_1	L_2	P_1	N_2	O_1	P_2	Q_1	O_2
	S_1	Q_2	R_1	S_2	T_1	R_2	V_1	T_2	U_1	V_2	W_1	U_2	Y_1	W_2	X_1	Y_2	Z_1	X_2
$b=15$	A_1	0	0	A_2	B_1	0	D_1	B_2	C_1	D_2	E_1	C_2	G_1	E_2	F_1			
	G_2	H_1	F_2	J_1	H_2	I_1	J_2	K_1	I_2	M_1	K_2	L_1	M_2	N_1	L_2			
	P_1	N_2	O_1	P_2	Q_1	O_2	S_1	Q_2	R_1	S_2	T_1	R_2	V_1	T_2	U_1			

agree with the rank values shown in Fig. 15. Moreover, it is to be noted that the difference between two successive columns with rank deficiency is equal to 6 (i.e. lcm(n, B)). Therefore, it has been inferred from Table 3 and Fig. 15 that if b is a multiple of lcm(n, B), then rank deficiency is obtained and $\rho(S) = \chi k + m + b - \chi n$ as mentioned in proposition 2. However, if b is not a multiple of lcm(n, B), then full rank is obtained as stated in proposition 2.

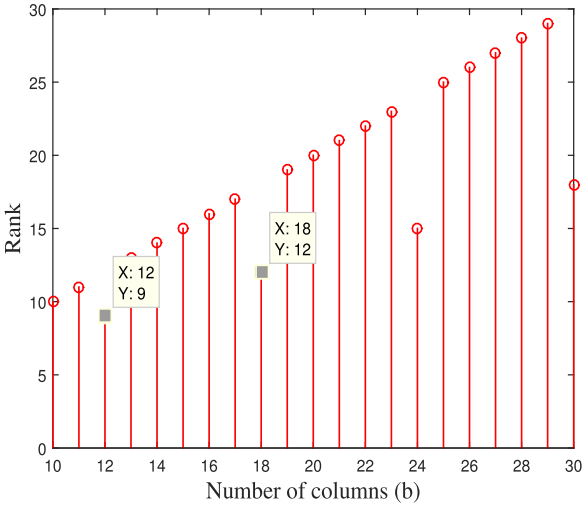

FIGURE 16. variation of rank with number of columns b for helical interleaver ($c(2, 1, 3)[5, 7]$, $c = 3$, $n = 2$, $d = 1$, $ber = 0$).

APPENDIX C
CASE STUDY 3: HELICAL INTERLEAVER

In this Appendix, the reason for rank deficiency considering the case when β is a multiple of n for helical interleaver has been explained using an example. Fig. 16 shows the variation of $\rho(S)$ with respect to b for helical interleaver assuming $C(2, 1, 3)[5, 7]$, $C = 3$, $N = 2$, and $d = 1$ considering non-erroneous and synchronized scenario. Similar to previous case studies, $\rho(S)$ for helical interleaver is computed using algorithm 1. In addition, the helical interleaved data stream considering $r = 1/2$ is reshaped into a matrix of size $a \times b$ with $a = 3$ and $b = 12$, 15, and 18 as shown in Table 4. Firstly, for the cases when $b = 12$ and $b = 18$, $\chi = 5$ and $\chi = 8$ complete continuous codewords, respectively, are observed in second and third rows aligned properly in the same column. This will result in rank deficiency and $\rho(S) = 9$ and 12 for $b = 12$ and $b = 18$, respectively assuming $K = 3$. This is because, after converting S into F, $\chi = 5$ complete continuous codewords that occupy 10 columns or χn columns in S will be converted into 7 or $\chi k + m$ non-zero columns in F through GJETP algorithm. Similarly, $\chi = 8$ complete codewords for the case when $b = 18$ will result in 10 non-zero columns. Already 2 independent columns (i.e. $b - \chi n$) are observed in S due to misalignment of codewords for both the cases. Therefore, the column echelon form of S will comprise of 9 and 12 non-zero columns for $b = 12$ and $b = 18$ cases, respectively or $\chi k + m + b - \chi n$ non-zero columns in general as mentioned in proposition 3. Since the number of non-zero columns in F gives the rank of a matrix, $\rho(S) = \chi k + m + b - \chi n$, which validates (1). It is also noticed from Table 4 that for the case when $b = 15$, all the 15 columns are observed to be independent due to misalignment of codewords and hence, it will result in full rank. Thus, the rank values evaluated from Table 4 assuming $K = 3$ well agree with the values shown in Fig. 16.

Since $\beta = C \times N$ is a multiple of n, rank deficiency is observed for the case when b is a multiple of β. For the case when b is not a multiple of β, full rank is observed as inferred from Table 4 and Fig. 16. Similar to case study 2, if b is not a multiple of β, rank deficiency will be observed for the case when b is a multiple of lcm(n, β). Further, full rank will be observed for rest of the cases.

REFERENCES

[1] G. Sicot, S. Houcke, and J. Barbier, "Blind detection of interleaver parameters," *Signal Process.*, vol. 89, no. 4, pp. 450–462, Apr. 2009.
[2] V. Kuvaja, "Identification of error correction codes in signals intelligence," M.S. thesis, School Elect. Eng., Aalto Univ., Espoo, Finland, 2015.
[3] J. F. Ziegler, "Automatic recognition and classification of forward error correcting codes," M.S. thesis, Dept. Elect. Comput. Eng., George Mason Univ., Fairfax, VA, USA, 2000.
[4] M. Marazin, R. Gautier, and G. Burel, "Blind recovery of k/n rate convolutional encoders in a noisy environment," *EURASIP J. Wireless Commun. Netw.*, vol. 2011, no. 168, pp. 1-9, Dec. 2016.
[5] M. Marazin, R. Gautier, and G. Burel, "Dual code method for blind recognition of convolutional encoder for cognitive radio receiver design," in *Proc. IEEE GLOBECOM*, Dec. 2009, pp. 1–6.
[6] *Digital Video Broadcasting (DVB); Framing Structure, Channel Coding and Modulation for Digital Terrestrial Television*, document ETSI EN 300 744 V1.5.1 (2004-06), Technical Specification ETSI, 2004.
[7] D. Hao and P. A. Hoeher, "Helical interleaver set design for interleave-division multiplexing and related techniques," *IEEE Commun. Lett.*, vol. 12, no. 11, pp. 843–845, Nov. 2008.
[8] D. Minoli, *Innovations in Satellite Communication and Satellite Technology*, Hoboken, NJ, USA: Wiley, 2015.
[9] N. Riaz and M. Ghavami, "An energy-efficient adaptive transmission protocol for ultrawideband wireless sensor networks," *IEEE Trans. Veh. Technol.*, vol. 58, no. 7, pp. 3647–3660, Sep. 2009.
[10] G. L. Rosen, "Examining coding structure and redundancy in DNA," *IEEE Eng. Med. Biol. Mag.*, vol. 25, no. 1, pp. 62–68, Jan. 2006.
[11] J. Dingel and J. Hagenauer, "Parameter estimation of a convolutional encoder from noisy observations," in *Proc. IEEE ISIT*, Jun. 2007, pp. 1776–1780.

[12] M. Marazin, R. Gautier, and G. Burel, "Some interesting dual-code properties of convolutional encoder for standards self-recognition," *IET Commun.*, vol. 6, no. 8, pp. 931–935, May 2012.
[13] M. Cluzeau and M. Finiasz, "Reconstruction of punctured convolutional codes," in *Proc. IEEE ITW*, Oct. 2009, pp. 75–79.
[14] M. Marazin, R. Gautier, and G. Burel, "Algebraic method for blind recovery of punctured convolutional encoders from an erroneous bitstream," *IET Signal Process.*, vol. 6, no. 2, pp. 122–131, Apr. 2012.
[15] Y. Zrelli, M. Marazin, E. Rannou, and R. Gautier, "Blind identification of convolutional encoder parameters over GF(2m) in the noiseless case," in *Proc. 20th IEEE ICCCN*, Aug. 2011, pp. 1–5.
[16] Y. Zrelli, R. Gautier, E. Rannou, M. Marazin, and E. Radoi, "Blind identification of code word length for non-binary error-correcting codes in noisy transmission," *EURASIP J. Wireless Commun. Netw.*, vol. 2015, no. 43, pp. 1–16, Dec. 2015.
[17] T. Xia and H.-C. Wu, "Novel blind identification of LDPC codes using average LLR of syndrome a posteriori probability," *IEEE Trans. Signal Process.*, vol. 62, no. 3, pp. 632–640, Feb. 2014.
[18] R. Moosavi and E. G. Larsson, "Fast blind recognition of channel codes," *IEEE Trans. Commun.*, vol. 62, no. 5, pp. 1393–1405, May 2014.
[19] P. Yu, H. Peng, and J. Li, "On blind recognition of channel codes within a candidate set," *IEEE Commun. Lett.*, vol. 20, no. 4, pp. 736–739, Apr. 2016.
[20] Y. G. Debessu, H.-C. Wu, and H. Jiang, "Novel blind encoder parameter estimation for turbo codes," *IEEE Commun. Lett.*, vol. 16, no. 12, pp. 1917–1920, Dec. 2012.
[21] P. Yu, J. Li, and H. Peng, "A least square method for parameter estimation of rsc sub-codes of turbo codes," *IEEE Commun. Lett.*, vol. 18, no. 4, pp. 644–647, Apr. 2014.
[22] L. Lu, K. H. Li, and Y. L. Guan, "Blind detection of interleaver parameters for non-binary coded data streams," in *Proc. IEEE ICC*, Jun. 2009, pp. 1–4.
[23] R. Swaminathan, A. S. Madhukumar, W. T. Ng, and C. M. S. See, "Parameter estimation of block and helical scan interleavers in the presence of bit errors," *Digit. Signal Process.*, vol. 60, pp. 20–32, Jan. 2017.
[24] L. Lu, K. H. Li, and Y. L. Guan, "Blind identification of convolutional interleaver parameters," in *Proc. 7th IEEE ICICS*, Dec. 2009, pp. 1–5.
[25] Y.-Q. Jia, L.-P. Li, Y.-Z. Li, and L. Gan, "Blind estimation of convolutional interleaver parameters," in *Proc. 8th IEEE WiCOM*, Sep. 2012, pp. 1–4.
[26] B. Sklar, *Digital Communications Fundamentals and Applications*, 2nd ed. Englewood Cliffs, NJ, USA: Prentice-Hall, 2001.
[27] *Helical Interleaver*, accessed on Apr. 5, 2017. [Online]. Available: http://www.mathworks.com/help/comm/ref/helicalinterleaver.html
[28] G. Golub and C. V. Loan, *Matrix Computations*, 3rd ed. Baltimore, MD, USA: Johns Hopkins Univ. Press, 1996.

SWAMINATHAN R received the B.Tech. degree in ECE from SASTRA University, Thanjavur, India, in 2009, the M.E. degree in communication systems from the College of Engineering Guindy, Anna University, Chennai, India, in 2011, and the Ph.D. degree from the Department of E&ECE, IIT Kharagpur, Kharagpur, India, in 2016. From 2011 to 2015, he was a Research Scholar with the Department of E&ECE, IIT Kharagpur. From 2015 to 2016, he was a Research Associate with the School of Computer Science and Engineering (SCSE), Nanyang Technological University. Since 2016, he has been a Research Fellow with SCSE. His current research interests are broadly in the performance analysis of wireless digital communication systems over fading channels, blind estimation of FEC code and interleaver parameters, cooperative communications, full-duplex relaying, energy harvesting communications, and visible light communications. He received the gold medal from the College of Engineering Guindy, Anna University. Furthermore, he has been serving as a Reviewer for internationally reputed journals and conferences.

A. S. MADHUKUMAR (SM'16) received the B.Tech. degree from the College of Engineering, Trivandrum, India, the M.Tech. degree from the Cochin University of Science and Technology, India, and the Ph.D. degree from the Department of Computer Science and Engineering, IIT Madras, Chennai, India. He is currently an Associate Professor with the School of Computer Engineering, Nanyang Technological University, Singapore.

He was involved in communications and signal processing research with the Centre for Development of Advanced Computing (Electronics R&D Centre), Government of India, and the Centre for Wireless Communications, Institute for Infocomm Research, Singapore. His research interests are in the areas of cooperative and cognitive radio systems, new modulation and multiple access schemes, and other advanced signal processing algorithms for communication systems. He is involved in a number of funded research projects, organizing international conferences, and is a Reviewer for many internationally reputed journals and conferences. He has authored over 200 referred international conference and journal papers.

NG WEE TECK received the B.Eng. and Ph.D. degrees from the School of Electrical and Electronic Engineering, Nanyang Technological University (NTU), Singapore, in 2001 and 2005, respectively, specialising in communication theory. He was with the Centre for Strategic Infocomm Technologies, Singapore, from 2004 to 2007. He is currently with DSO National Laboratories, Singapore. He has been adjunct to Temasek Labs, NTU, as a Senior Research Scientist, since 2008.

CHONG MENG SAMSON SEE (M'92) received the Diploma degree (Hons.) in electronics and communications engineering from Singapore Polytechnic in 1988, and the M.Sc. degree in digital communication systems and the Ph.D. degree in electrical engineering from the Loughborough University of Technology, Loughborough, U.K., in 1991 and 1999, respectively. Since 1992, he has been with DSO National Laboratories, Singapore, where he is currently a Distinguished Member of the Technical Staff and leading a team in the research and development of advanced array signal processing systems and algorithms. He also holds an adjunct appointment with Temasek Laboratories, Nanyang Technological University, as a Principal Research Scientist. He played a key role in the research and development of statistical and array signal processing for defence applications. In recognition of his contributions to defence R&D, he received the Defence Technology Prize 2015 Individual R&D Award and the Defence Technology Prize 2014 Engineering Award. He has two issued patents on direction finding. His research interests include the area of statistical and array signal processing, communications, and bio-inspired systems. He is currently a member of the IEEE Sensor Array and Multichannel Signal Processing Technical Committee. He was an Associate Editor of the IEEE TRANSACTIONS ON SIGNAL PROCESSING.